Magnetic ordering in the ammoniated alkali fullerides $(NH_3)K_{3-x}Rb_xC_{60}$ (x = 2, 3)

2007 J. Phys.: Condens. Matter 19 386235

(http://iopscience.iop.org/0953-8984/19/38/386235)

J. Phys.: Condens. Matter **19** (2007) 386235 (13pp) doi:10.1088/0953-8984/19/38/386235

Magnetic ordering in the ammoniated alkali fullerides $(NH_3)K_{3-x}Rb_xC_{60}$ ($x = 2, 3$)

J Arvanitidis[1,2], K Papagelis[3], Y Takabayashi[4], T Takenobu[5], Y Iwasa[5], M J Rosseinsky[6] and K Prassides[4]

[1] Physics Division, School of Technology, Aristotle University of Thessaloniki, 54124 Thessaloniki, Greece
[2] Department of Applied Sciences, Technological Educational Institute of Thessaloniki, 57400 Sindos, Greece
[3] Materials Science Department, University of Patras, 26504 Patras, Greece
[4] Department of Chemistry, University of Durham, Durham DH1 3LE, UK
[5] Institute for Materials Research, Tohoku University, 2-1-1 Katahira, Aoba-ku, Sendai 980-8577, Japan
[6] Department of Chemistry, University of Liverpool, Liverpool L69 7ZD, UK

E-mail: K.Prassides@durham.ac.uk

Received 24 May 2007, in final form 14 August 2007
Published 4 September 2007
Online at stacks.iop.org/JPhysCM/19/386235

Abstract

In this work, we present a detailed study of the ammoniated fullerides $(NH_3)KRb_2C_{60}$ and $(NH_3)Rb_3C_{60}$ using the μ^+ spin relaxation/rotation (μ^+SR) technique in its zero-field (ZF), longitudinal-field (LF) and transverse-field (TF) variants as a function of temperature and cooling rate. The ZF and TF μ^+SR spectra of the investigated ammoniated alkali fullerides clearly reveal the onset of long-range antiferromagnetic (AF) order at low temperatures. In the AF state, the local field exhibits large spatial inhomogeneities, while its quasi-static nature is confirmed by the complete recovery of the asymmetry in an LF of 200–500 Oe. A large fraction of paramagnetic domains survives well into the AF state. In addition, the cooling rates of the samples affect sensitively the coherent ordering of the magnetic moments, while the Néel temperature T_N remains essentially unchanged. Finally, the anomalous evolution of the Néel temperatures with x across the $(NH_3)K_{3-x}Rb_xC_{60}$ ($0 \leqslant x \leqslant 3$) series is ascribed to the different low-temperature orientationally ordered superstructures appearing between $x = 2$ and 3.

(Some figures in this article are in colour only in the electronic version)

1. Introduction

Superconducting transition temperatures, T_c, are as high as 33 K at ambient pressure for chemically intercalated fulleride salts [1], rising to 40 K at elevated pressures [2]. Despite the apparent simplicity of fullerene-based materials, certain features of their electronic properties,

including the comparable magnitudes of the Fermi and phonon energies and the role of electron correlations, have attracted considerable interest [3–6]. The metallic nature of cubic A_3C_{60} fullerides has been rationalized in terms of the triple orbital degeneracy of the lowest unoccupied molecular orbital (LUMO) t_{1u} states. It was shown that when the on-site Coulomb repulsion, U, is smaller than $\sim 2.5W$, where W is the t_{1u} bandwidth, no transition to a Mott–Hubbard insulator occurs and metallic behaviour is observed [7]. Noting that W in fullerides depends sensitively on the interfullerene separation, a transition to a Mott insulating state is anticipated when electron correlation effects become dominant. This may occur when the degeneracy of the t_{1u} orbitals is removed through lowering of the crystal symmetry (the critical U/W ratio, $(U/W)_c$, decreases to values lower than 2.5) and/or the interfullerene separation increases sufficiently for U/W to exceed the critical value $(U/W)_c$.

$(NH_3)K_3C_{60}$, obtained by the introduction of one ammonia molecule in the octahedral site of the cubic structure of K_3C_{60}, has been a key compound for the understanding of the metal–insulator (MI) transition at large interfullerene spacings. Ammoniation is accompanied by an anisotropic expansion of the fulleride structure and a reduction in crystal symmetry to orthorhombic [8]. The nature of the electronic state of $(NH_3)K_3C_{60}$ at high temperature was originally controversial. While early magnetic susceptibility, electron paramagnetic resonance (EPR) and ^{13}C nuclear magnetic resonance (NMR) measurements described it as a narrow band metal [9–11], it has been subsequently shown by microwave conductivity [12] and ^{13}C NMR studies [13] that it is an insulator. On the other hand, there is universal agreement that, below $\sim$40 K, the electronic ground state is that of a long-range ordered antiferromagnet (LRO-AF) with a staggered magnetic moment of the order of 1 μ_B/C_{60} molecule [11–14]. In particular, zero-field muon spin relaxation (ZF μ^+SR) studies showed that the temperature evolution of the internal magnetic fields below T_N follows closely the behaviour of a conventional three-dimensional (3D) Heisenberg antiferromagnet [14]. $(NH_3)K_3C_{60}$ also undergoes a structural transition below $T_S = 150$ K, driven by the orientational ordering of both the K^+–NH_3 pairs (antiferroelectric, AFE, ordering) [15] and the C_{60} units [16]. In addition, there exists a remarkable correlation of the C_{60} ordering motif and the 3D AF structure proposed by NMR [13] with the intermolecular magnetic exchange interactions sensitively depending on the relative orientation of near-neighbour C_{60} units [16].

Of particular interest have been also attempts to increase the interfullerene separation even further by synthesizing the $(NH_3)K_{3-x}Rb_xC_{60}$ ($x = 1$, 2, and 3) solid solutions. These are isostructural with $(NH_3)K_3C_{60}$ at room temperature, and EPR studies showed again the presence of low-temperature magnetic transitions [17]. The derived T_N first increases with increasing interfullerene spacing up to 76 K for $x = 2$ and then decreases to 58 K for $x = 3$, an observation which was rationalized in terms of the Mott–Hubbard model in which there is a crossover from itinerant ($x = 0$, 1, 2) to localized ($x = 3$) behaviour with increasing U/W [18]. Noticeably, the observed variation of T_N with interfullerene separation is in sharp contrast to what is expected for a simple localized moment model—a smooth decrease in the exchange interaction, J and the Néel temperature, T_N, with increasing lattice constant—despite the experimental evidence that all members of the $(NH_3)K_{3-x}Rb_xC_{60}$ series are insulating over the whole temperature range [12].

In this paper, we report a detailed study of the ammoniated fullerides $(NH_3)K_{3-x}Rb_xC_{60}$ ($x = 2, 3$) with the ZF μ^+SR technique, which is extremely powerful in cases of small-moment magnetism and in all instances where magnetic order is of a random, very short-range, spatially inhomogeneous or incommensurate nature [19]. The transitions to LRO antiferromagnetic states are authenticated for both compounds, but quasi-static spin freezing is observed at significantly lower temperatures ($\sim$54 K and $\sim$51 K for $x = 2$ and 3, respectively) than those reported by EPR [17]. Rapid cooling through the orientational ordering transition leads

to considerable enhancement of the spatial inhomogeneities in the local fields experienced by the muons, demonstrating the sensitivity of the fullerene exchange interactions to the relative orientations of near-neighbour units. Muon spin rotation (TF μ^+SR) measurements at an applied field of 6 kOe also show the onset of magnetic order, but at somewhat higher temperature.

2. Experimental details

The $(NH_3)Rb_3C_{60}$ and $(NH_3)KRb_2C_{60}$ samples used in the present work were prepared by reaction of stoichiometric amounts of C_{60} and the appropriate alkali metals with liquid ammonia, as described before [17]. Phase purity was confirmed by synchrotron x-ray diffraction with the high-resolution powder diffractometer on beamline ID31 at the European Synchrotron Radiation Facility (ESRF), Grenoble, France. Zero-field (ZF), longitudinal-field (LF = 200–500 Oe), and transverse-field (TF = 6 kOe) μ^+SR data were collected at the Paul Scherrer Institute (PSI), Villigen, Switzerland, with the general-purpose spectrometer (GPS) using low-energy (surface) muons on the μ^+SR dedicated πM3 beamline of the PSI 600 MeV proton accelerator. The powder samples (90–180 mg) were sealed under argon in silver sample holders equipped with indium seals and Mylar windows, and placed inside a continuous-helium cryostat operating in the temperature range 1.7–310 K. The samples were first cooled from ambient temperature at different rates (0.6 and 2.8 K min^{-1} for $(NH_3)Rb_3C_{60}$ and 1.8 K min^{-1} for $(NH_3)KRb_2C_{60}$) and the μ^+SR measurements were then performed on heating.

In a μ^+SR experiment, 100% spin-polarized positive muons are implanted in the sample. After coming to rest at an interstitial lattice site, they can act as highly sensitive microscopic local magnetic probes, since, under the influence of internal static and dynamic fields, their polarization becomes time dependent. The time evolution of the μ^+ spin polarization, $P_\mu(t)$, can be monitored by recording time histograms of the muon-decay positrons emitted preferentially along the μ^+ spin direction. In the presence of local internal or external magnetic fields, $\langle B_\mu \rangle$, the muons undergo Larmor precession with a frequency given by $\nu_\mu = (\gamma_\mu/2\pi)\langle B_\mu \rangle$, where $\gamma_\mu/2\pi = 13.553$ kHz G^{-1} is the muon gyromagnetic ratio. In the absence of an applied external field (ZF), the appearance of a precession in $P_\mu(t)$ signals the onset of an ordering (ferromagnetic or antiferromagnetic) transition. Moreover, application of a magnetic field parallel to the initial μ^+ spin polarization (LF) allows the decoupling of the μ^+ spin from static internal fields.

3. Results and discussion

3.1. Zero-field muon spin relaxation in $(NH_3)Rb_3C_{60}$ after slow cooling

In figure 1(a), we show the ZF time-dependent μ^+SR spectra of $(NH_3)Rb_3C_{60}$ at 2 and 60 K, measured on heating after slow cooling the sample at 0.6 K min^{-1} to low temperatures. No oscillating signal is seen at 60 K and the μ^+SR spectrum is characteristic of the presence of weak static nuclear dipole moments, which result in a small depolarization rate, $\sigma \approx 0.05\ \mu s^{-1}$. This muon relaxation arises principally from the hydrogen nuclear moments, which are frozen into a disordered spin configuration, producing a distribution of local fields with a width $\langle \Delta B^2 \rangle^{1/2} \approx 0.6$ Oe. However, an additional slow relaxation of the μ^+ spin polarization is also present, arising from fluctuating electronic moments. Thus the spectrum was fitted with the product of a Gaussian (σ) and an exponential (λ_d) relaxation, the latter accounting for the moments of the C_{60}^{3-} units, while keeping the amplitude A fixed to the value determined by weak TF measurements at room temperature. The relaxation rate, λ_d, is 0.042(3) μs^{-1}, and a

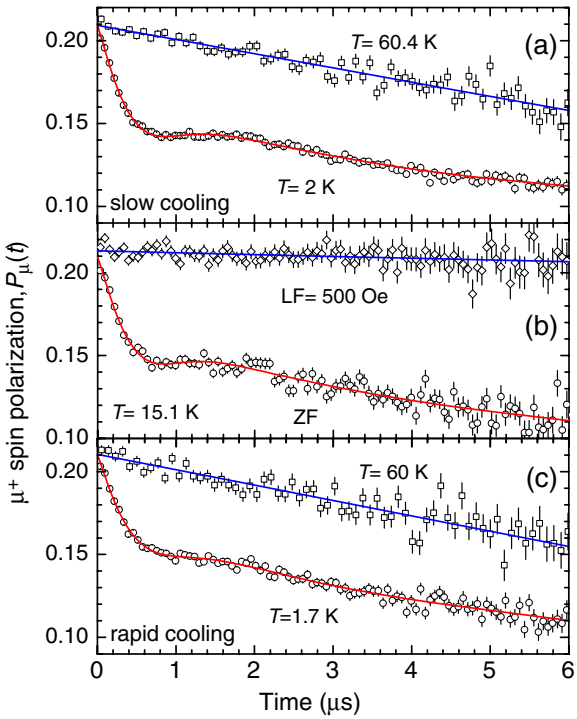

Figure 1. Evolution of the ZF μ^+ spin polarization, $P_\mu(t)$ at low (circles) and higher (squares) temperatures in $(NH_3)Rb_3C_{60}$ after (a) slow and (c) rapid cooling. (b) Evolution of $P_\mu(t)$ at ZF (circles) and LF = 500 Oe (squares) for the slowly cooled sample at 15 K. The solid lines through the experimental points are fits using the functions given in the text.

rough estimate of the fluctuation rate, $\nu \sim 10^9$ Hz (just before freezing), can be calculated by assuming an average transverse component of the field strength (*vide infra*) of 40 Oe.

At lower temperatures (figure 1(a)) the ZF μ^+SR spectra are dominated by a short-lived component whose depolarization gradually increases with decreasing temperature. In addition, their shape is very similar to that observed in related fulleride salts, such as $(NH_3)K_3C_{60}$ [14] and $(TDAE)C_{60}$ [20]. For instance, there is no long-lived oscillating component evident even in the high-statistics data at 2 K. Instead, the asymmetry decays rapidly at time $t < 0.6$ μs, shows a minimum between 0.6 and 0.8 μs, and recovers at $t > 0.8$ μs. At long times ($t \gg 1.5$ μs), it continues to relax at an increasing rate with increasing temperature. These characteristics are similar to the features of the dynamic Kubo–Toyabe relaxation function [21, 22], appropriate for a Gaussian distribution of random fields whose rate decreases with decreasing temperature. Even though this function could provide an appealing description of the low-temperature magnetic phase, it is inappropriate on the evidence of complementary μ^+SR data collected at low temperatures in a field of 500 Oe, which reveal a complete recovery of the asymmetry (figure 1(b)). As the effect of applied LFs is the decoupling of the depolarization due to dynamic or fluctuating moments from that due to static components, we conclude that the dynamic Kubo–Toyabe description of the ZF μ^+SR data (which necessitates the presence of fluctuating random fields with rates in excess of 0.5 μs^{-1}) is inappropriate and the origin of the observed relaxation in ZF is quasi-static in nature.

We thus explored the fitting of the data at low temperatures with a strongly damped oscillating function superimposed on a slowly relaxing component. The solid line in figure 1(a)

is a fit to the data of the function

$$P_\mu(t) = A_1\{(1/3)\exp(-\tfrac{1}{2}\sigma_1^2 t^2) + (2/3)\exp(-\lambda_1 t\cos(2\pi\nu_\mu t))\} + A_2\exp(-\tfrac{1}{2}\sigma_2^2 t^2), \quad (1)$$

where A_1 and A_2 are amplitudes reflecting the fractions of the muons contributing to the two components, $\nu_\mu = \omega_\mu/2\pi$ is the μ^+ Larmor precession frequency, and λ_1, σ_1, and σ_2 are relaxation rates associated with the two components. The physical origin of the first term in equation (1) lies with the fact that, on average, for a completely random distribution of the directions of the internal field in a polycrystalline sample, 1/3 of all muons will experience an internal field along their initial spin direction and consequently they will not precess. The relaxation of this 1/3-term is normally due to fluctuating field components perpendicular to the μ^+ spin and is typically described by an exponential. Unusually, in the present case, where the LF data also reveal purely static behaviour, the damping of the 1/3-term is best fitted by a Gaussian function. On the other hand, the damping of the oscillating term in equation (1) reflects the influence of static field inhomogeneities, which lead to loss of phase coherence of the precessing muons.

As already mentioned, the appearance of the oscillating signal in the ZF μ^+SR spectra evidences the existence of coherent ordering of the electronic spins and underlines the long-range AF ordering at lower temperatures ($T \leqslant T_N$), while the strong oscillation damping is the signature of spatial disorder and inhomogeneity effects. The first two terms in equation (1) are related to the AF component. The spontaneous oscillating signal is described by the second term of the fitting function. The exponential relaxation rate, λ_1, refers to μ^+ spin depolarization due to both static and dynamic field inhomogeneities parallel to the spontaneous field direction. At 2 K, the μ^+ spin precession frequency, ν_μ, related with the coherent ordering of the electronic spins, is 0.48(1) MHz, corresponding to a static local field at the μ^+ site, $\langle B_\mu\rangle = 35.7(7)$ Oe. At this temperature we find that $\lambda_1 = 2.63(8)$ μs^{-1}, implying a distribution of the local fields with a width $\langle\Delta B^2\rangle^{1/2} = 30.9(9)$ Oe (where $\langle\Delta B^2\rangle^{1/2} = \lambda_1/\gamma_\mu$ [23]). Similar $\langle B_\mu\rangle$ and $\langle\Delta B^2\rangle^{1/2}$ values have been obtained earlier for $(NH_3)K_3C_{60}$ [14, 24]. The comparable values for $\langle B_\mu\rangle$ and $\langle\Delta B^2\rangle^{1/2}$ reveal the large spatial inhomogeneities of the local field in the AF state of the ammoniated alkali fullerides, resulting from a number of physical reasons such as the orientational disordering of the C_{60} molecular cages. Finally, the slowly relaxing component (third term in equation (1)) is connected with the existence of paramagnetic (PM) domains in the AF state of the studied compound even at the lowest temperatures attained in our measurements.

Figure 2 shows the temperature dependence of the μ^+ spin precession frequency, ν_μ, obtained in $(NH_3)Rb_3C_{60}$ at zero external field. The $\nu_\mu(T)$ data were best described above 25 K using the formula

$$\nu_\mu = \nu_0\{1 - (T/T_N)\}^\beta \quad (2)$$

with $\nu_0 = 0.54(1)$ MHz, $T_N = 51(1)$ K and $\beta = 0.36(12)$. The theoretical value of the critical exponent for a 3D Heisenberg system is 0.367 [25], while the experimental values for various isotropic 3D antiferromagnets range between 0.3 and 0.4 [26]. Thus, the temperature dependence of the μ^+ precession frequency due to the local fields in the AF state of $(NH_3)Rb_3C_{60}$ is consistent with that of a conventional 3D Heisenberg antiferromagnet. This result is similar to that obtained by the ZF μ^+SR technique for $(NH_3)K_3C_{60}$ ($\beta = 0.32(3)$, $\nu_0 = 0.64(1)$ MHz, and $T_N = 36.5(3)$ K) [14]. By comparing the frequency at zero temperature, ν_0, obtained for $(NH_3)Rb_3C_{60}$ with that of the $(TDAE)C_{60}$ (0.92 MHz) ferromagnet [20], which exhibits a magnetic moment of $\mu(0\,K) \sim 1\ \mu_B$/molecule, and by assuming similar μ^+ stopping sites for the two systems (although for powder samples the exact μ^+ site is not known, it is expected that this will reside near the C_{60}^{3-} anions), we estimate $\mu(0\ K) \sim 0.6\ \mu_B$/molecule in $(NH_3)Rb_3C_{60}$, comparable with that obtained for $(NH_3)K_3C_{60}$ ($\sim$0.7 μ_B/molecule) [14].

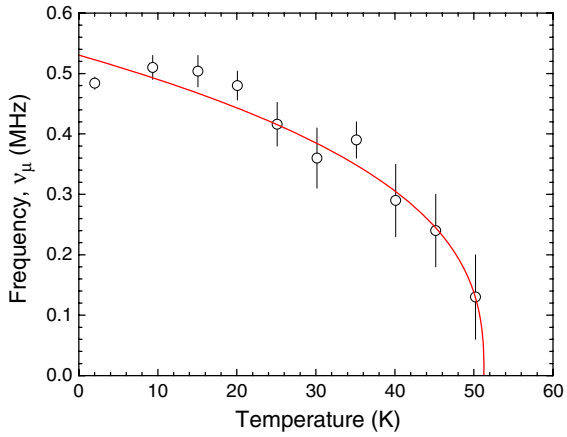

Figure 2. Temperature dependence of the ZF μ^+ spin precession frequency, ν_μ, in $(NH_3)Rb_3C_{60}$. The solid line is a fit to the data of the function given in the text.

Moreover, in $(NH_3)Rb_3C_{60}$ the relaxation rate λ_1, which is related to the short-lived oscillating AF term, displays a similar temperature dependence to that of ν_μ, namely it decreases almost quadratically as the temperature increases, reaching the value of 1.8(3) μs^{-1} at $T = 50$ K (figure 3(a), open circles). On the other hand, the Gaussian relaxation rate, σ_1, remains almost constant with temperature, having an average value of 0.47 μs^{-1} (figure 3(a), open squares). Finally, σ_2 (related to the PM domains in the AF state) smoothly increases with temperature from 0.064(5) μs^{-1} at 2 K to 0.10(2) μs^{-1} at 50 K.

The inset in figure 3(a) illustrates the temperature dependence of the estimated volume fraction of the antiferromagnetically ordered component $[=A_1/(A_1 + A_2) \times 100\%]$ in $(NH_3)Rb_3C_{60}$ after slow cooling. As the temperature decreases below T_N, the fraction of the magnetically ordered domains grows at the expense of the paramagnetic ones, reaching a value of 42.9(5)% at 2 K. This may reflect the presence of different exchange constants (different ordering temperatures), arising from the orientational disorder of the C_{60}^{3-} units. The coexistence—even at the lowest temperatures—of paramagnetic and magnetically ordered domains and the relatively small value of the AFM fraction point towards an inhomogeneous form of magnetism in this compound.

3.2. Effect of cooling protocol on the AF ordering in $(NH_3)Rb_3C_{60}$

The evolution of the ZF $P_\mu(t)$ at low (circles) and higher (squares) temperatures in $(NH_3)Rb_3C_{60}$ after rapid cooling is presented in figure 1(c). Fitting of the μ^+SR spectrum at 1.7 K using equation (1) results in $\nu_\mu = 0.42(3)$ MHz and $\lambda_1 = 2.6(2)$ μs^{-1}, corresponding to $\langle B_\mu \rangle \approx \langle \Delta B^2 \rangle^{1/2} \approx 31$ Oe and revealing a $\langle \Delta B^2 \rangle^{1/2} / \langle B_\mu \rangle$ ratio even larger than that obtained on slow cooling. Moreover, above 10 K, the short-lived oscillating component essentially disappears and only a fast depolarization of the μ^+ spin is evident, showing the suppression of the magnetic ordering in the AF state of the fulleride. In $(NH_3)K_3C_{60}$, it has been found that the intermolecular exchange interactions depend sensitively on the relative orientation of the neighbouring C_{60} anions [16]. The orientational order/disorder of the molecular cages results in different relative orientations of the molecular orbitals and therefore different overlap of the electronic wavefunctions that modulates the intermolecular exchange interactions. Thus, the possible explanation for the significant attenuation of the coherent ordering of the electronic

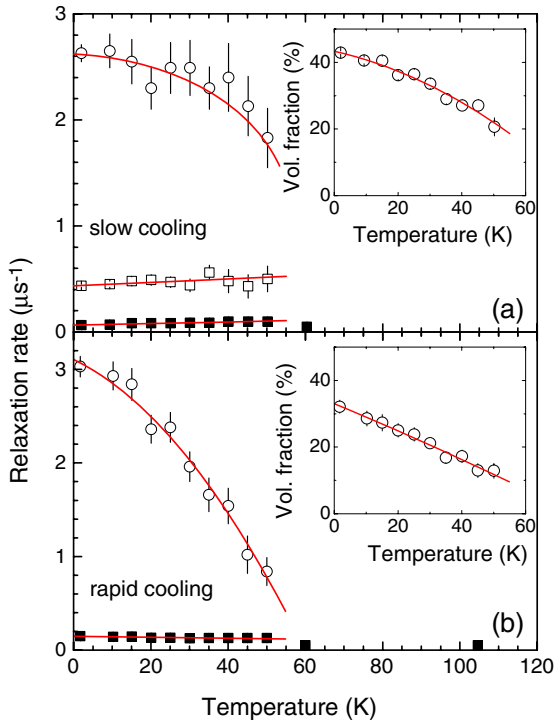

Figure 3. Temperature dependence of the depolarization rates for the magnetically ordered (σ_1 (open squares) and λ_1 (open circles)) and the paramagnetic (σ_2, solid squares) components of $(NH_3)Rb_3C_{60}$ after (a) slow and (b) rapid cooling. The insets show the temperature dependence of the volume fraction of the antiferromagnetically ordered component in this ammoniated fulleride. The solid lines through the data are guides to the eye.

spins after rapid cooling of the $(NH_3)Rb_3C_{60}$ sample is the consequent quenching of the orientational disorder of the C_{60} units. However, rapid cooling of the sample does not affect the onset temperature of spin freezing. The ZF μ^+SR data at temperatures above 10 K were fitted with a heavily damped exponential function (AF ordered domains) superimposed on the Gaussian component due to the quasi-static nuclear moments (PM domains):

$$P_\mu(t) = A_1 \exp(-\lambda_1 t) + A_2 \exp(-\tfrac{1}{2}\sigma_2^2 t^2). \tag{3}$$

At $T = 1.7$ K, we obtain $\lambda_1 = 3.0(1)$ μs^{-1}, implying a non-zero field spread of $\langle \Delta B^2 \rangle^{1/2} = 36(1)$ Oe. Thus, the muons experience a local field with a Lorentzian distribution that peaks close to zero, exhibiting large spatial inhomogeneities. As the temperature increases above 1.7 K, the Lorentzian relaxation rate, λ_1, decreases almost quadratically, reaching 0.8(2) μs^{-1} at 50 K (figure 3(b), open circles). The Gaussian relaxation rate σ_2 remains essentially constant in the whole temperature range of the AF state of the material, with a mean value of 0.14 μs^{-1} (figure 3(b), solid squares). In addition, we find that the volume fraction of the AF component in $(NH_3)Rb_3C_{60}$ after rapid cooling reaches 32(2)% at 1.7 K (inset in figure 3(b)), significantly smaller than that obtained in the same sample following slow cooling. This result indicates that the cooling rate also plays an important role in the relative concentration of magnetically ordered and paramagnetic domains. Finally, the quasi-static nature of the local field in the AF state of the rapidly cooled sample has been also confirmed by the complete recovery of the asymmetry at LF = 200 Oe ($\lambda = 0.010(2)$ μs^{-1}).

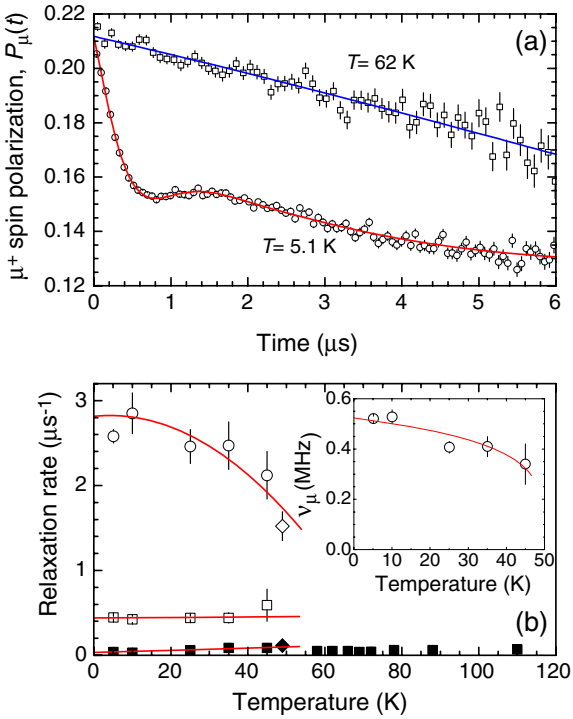

Figure 4. (a) Evolution of the ZF μ^+ spin polarization, $P_\mu(t)$, at low (circles) and higher (squares) temperatures in $(NH_3)KRb_2C_{60}$. The solid lines through the experimental points are fits using the functions given in the text. (b) Temperature dependence of the depolarization rates for the magnetically ordered (σ_1 (open squares) and λ_1 (open circles and diamond)) and the paramagnetic (σ_2, solid squares and diamond) components. The inset shows the temperature dependence of the ZF μ^+ spin precession frequency, ν_μ. The solid lines through the data are guides to the eye.

3.3. AF ordering in $(NH_3)KRb_2C_{60}$

Figure 4(a) illustrates the time evolution of the ZF μ^+ spin polarization for the $(NH_3)KRb_2C_{60}$ sample. As in the case of $(NH_3)Rb_3C_{60}$, the ZF μ^+SR data for $(NH_3)KRb_2C_{60}$ at higher temperatures (above T_f) were fitted using a double relaxation function (the product of a Gaussian and an exponential function). The results obtained reflect again the presence of weak quasi-static hydrogen nuclear magnetic moments distributed with an average width of $\langle \Delta B^2 \rangle^{1/2} = 0.63$ Oe in the temperature range 58–200 K. Moreover, $\lambda = 0.009(2)\ \mu s^{-1}$ at 200 K, equivalent to a fluctuating rate of the electronic moments $\nu \sim 1.5 \times 10^9$ Hz. Cooling leads to a slowing down of the electron spin dynamics within the PM domains, and λ approaches $0.033(2)\ \mu s^{-1}$ ($\nu \sim 4 \times 10^8$ Hz) at $T = 58$ K. The fitting of the exponential relaxation rate data in the temperature range 58–200 K with the critical law $\lambda = \lambda_0\{T/(T - T_f)\}^\alpha$ gives a value of the freezing temperature $T_f \sim 54$ K ($\alpha \sim 0.5$).

Below T_f, a short-lived heavily damped oscillating component appears again in the μ^+SR spectra (reflecting the onset of long-range AF ordering) in addition to the remaining slowly relaxing component. Therefore, we have also used equation (1) to fit the data in the low-temperature regime. At 5 K, we find that $\nu_\mu = 0.521(9)$ MHz, corresponding to $\langle B_\mu \rangle = 38.5(7)$ Oe, while $\lambda_1 = 2.58(8)\ \mu s^{-1}$, corresponding to $\langle \Delta B^2 \rangle^{1/2} = 30.3(9)$ Oe.

The ratio $\langle \Delta B^2 \rangle^{1/2} / \langle B_\mu \rangle$ is again close to unity, reflecting the large spatial inhomogeneities of the local field.

Figure 4(b) illustrates the temperature dependence of the μ^+ spin depolarization rates and its precession frequency in $(NH_3)KRb_2C_{60}$. With increasing temperature, ν_μ and the exponential relaxation rate λ_1 (open circles)—associated with field inhomogeneities along the μ^+ spin direction—decrease, reaching values of 0.34(8) MHz and 2.1(3) μs^{-1}, respectively, at 45 K. As in the case of $(NH_3)Rb_3C_{60}$, σ_1 (open squares), measuring local field inhomogeneities perpendicular to the μ^+ spin polarization, remains essentially temperature independent with a mean value of 0.47 μs^{-1}. In addition, the Gaussian relaxation rate, σ_2 (solid squares), of the PM component in equation (1) increases slightly with temperature from 0.039(7) μs^{-1} at 5 K to 0.09(1) μs^{-1} at 45 K. Finally, we note that, as the oscillating signal considerably weakens at $T = 49$ K, we reverted to the simplified function of equation (3) to fit the ZF μ^+SR spectrum (figure 4(b), diamonds). At this temperature, we find that $\lambda_1 = 1.5(2)$ μs^{-1} and $\sigma_2 = 0.115(5)$ μs^{-1}.

The estimated volume fraction of the AF domains in $(NH_3)KRb_2C_{60}$ also shows a comparable temperature dependence to that in $(NH_3)Rb_3C_{60}$—namely, it increases with decreasing temperature, reaching only 37.2(3)% at 5 K. Moreover, complementary measurements at LF = 200 Oe lead to complete recovery of the asymmetry (only a small relaxation rate, $\lambda = 0.006(2)$ μs^{-1}, survives) and confirm the quasi-static nature of the local fields.

3.4. TF μ^+SR measurements on $(NH_3)KRb_2C_{60}$

μ^+ spin rotation data at an applied TF of 6 kOe were also collected for the $(NH_3)KRb_2C_{60}$ fulleride between 1.7 K and ambient temperature. At high temperatures, the μ^+SR spectra can be fitted by using the single oscillating Gaussian function:

$$P_\mu(t) = A \exp(-\tfrac{1}{2}\sigma t^2) \cos(2\pi \nu_\mu t + \phi). \tag{4}$$

The relaxation rate, σ, is essentially temperature independent with an average value of 0.08(1) μs^{-1}, reflecting again the nuclear dipole field spread as in ZF. Below 60 K, a second rapidly relaxing component appears in the spectra with a depolarization rate that smoothly increases with decreasing temperature. This again provides the signature of the onset of spin freezing as in the ZF experiments. Therefore, at lower temperatures the TF μ^+SR spectra were best described by the function

$$P_\mu(t) = A_1 \exp(-\tfrac{1}{2}\sigma_1^2 t^2) \cos(2\pi \nu_\mu t + \phi_1) + A_2 \exp(-\tfrac{1}{2}\sigma_2^2 t^2) \cos(2\pi \nu_\mu t + \phi_2). \tag{5}$$

Figure 5 presents the temperature dependence of the relative shift in the μ^+ spin precession frequency, ν_μ, and the relaxation rates, σ_1 (solid squares) and σ_2 (open circles), of the two Gaussian components extracted by fitting the spectra to equation (5). As the temperature decreases, the relaxation rate of the slowly relaxing component, σ_1, slightly increases from 0.07(2) μs^{-1} at 60 K to 0.158(4) μs^{-1} at 1.7 K. On the other hand, the relaxation rate, σ_2, of the heavily damped component increases rapidly with decreasing temperature ($\sigma_2 = 0.41(9)$ μs^{-1} at 60 K and 2.04(2) μs^{-1} at 1.7 K), mimicking the behaviour of the corresponding component present in the ZF μ^+SR spectra. This response is accompanied by a concomitant increase in the relative fraction of the heavily damped component (inset in figure 5(b)). The volume fraction of the antiferromagnetically ordered domains reaches 41(6)% at 1.7 K, close to the value obtained from the ZF μ^+SR analysis.

The onset of the electronic spin freezing transition is also evident in the temperature dependence of the relative shift of the μ^+ spin precession frequency, ν_μ (figure 5(a)). On cooling below room temperature, the relative frequency shift remains essentially constant

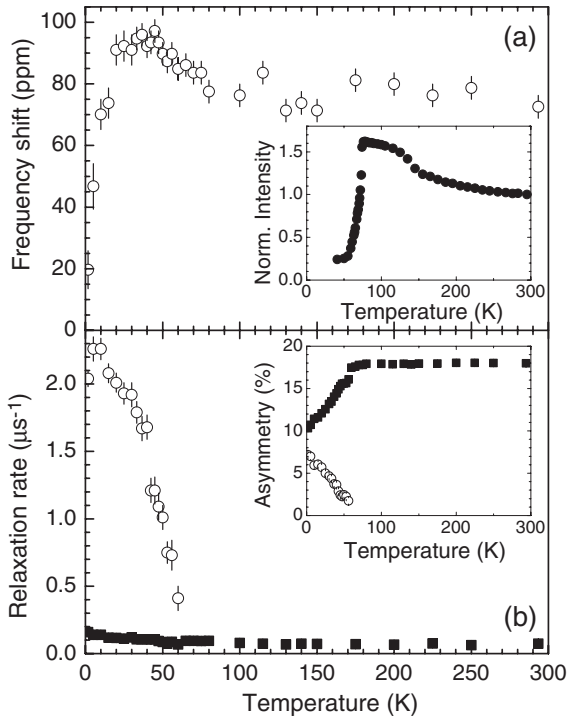

Figure 5. Temperature dependence of (a) the relative shift in the μ^+ spin precession frequency, ν_μ and (b) the relaxation rates of the two Gaussian, σ_1 (solid squares) and σ_2 (open circles), components present in the TF μ^+SR spectra of $(NH_3)KRb_2C_{60}$. The inset in (a) shows the temperature dependence of the integrated intensity (normalized by the room-temperature value) for the EPR signal [17], while the inset in (b) shows the asymmetries A_1 (solid squares) and A_2 (open circles) of the two Gaussian components.

down to ∼80 K, and then increases smoothly until ∼50 K. Below this temperature, it starts to decrease, while below 20 K the trend becomes very abrupt. The inset in figure 5(a) shows the temperature dependence of the spin susceptibility, χ_s, of $(NH_3)KRb_2C_{60}$ as extracted from the integrated intensity of the EPR signal [17]. There is a similar overall behaviour with the ν_μ shift data reflecting the behaviour of χ_s, but the scaling is not precise and the onset of the magnetic transition is shifted to lower temperature in the TF μ^+SR experiment.

3.5. Evolution of the Néel temperature in the $(NH_3)K_{3-x}Rb_xC_{60}$ series

The T_N values of the $(NH_3)K_{3-x}Rb_xC_{60}$ samples have been estimated from the ZF μ^+SR data as ∼54 K for $x = 2$ and ∼51 K for $x = 3$, while the TF μ^+SR measurements give a $T_N \sim 60$ K for $x = 2$. These values are considerably smaller than those reported for these fullerides by EPR experiments at 9.6 GHz [17], in contrast to the $x = 0$ [14] system where a comparable ordering temperature of ∼40 K was found by both techniques. This is an intriguing observation meriting further investigation, and it implies a rather unusual nature of the AF transition in the larger ammoniated alkali fullerides and the possibility that the onset of magnetic ordering shows a sensitive dependence on the time window of the experimental technique. Moreover, the μ^+SR experiments on the $x = 2$ and 3 samples reveal a sensitivity of the spin freezing of the C_{60}^{3-} ions both to the rate of cooling (rapid cooling leads to a significantly more disordered

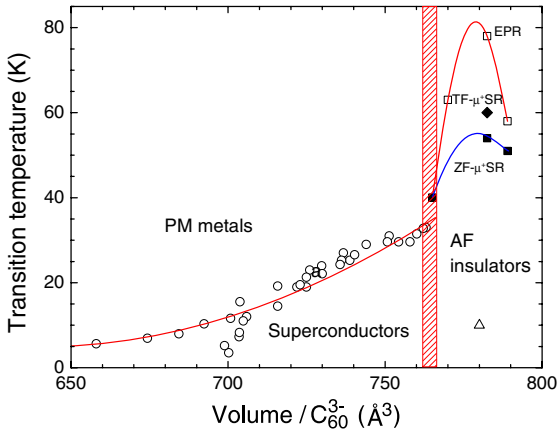

Figure 6. Electronic phase diagram of C_{60}^{3-} compounds including the T_c literature values for various superconducting fullerides (open circles) and the T_N values for $(NH_3)K_{3-x}Rb_xC_{60}$ (open squares from EPR measurements [17] and solid squares and diamond from ZF and TF μ^+SR spectra, respectively) and $(CH_3NH_2)K_3C_{60}$ (triangle) [30]. The shaded area denotes the metal (PM)–insulator (AF) boundary.

form of magnetism due to orientational disorder) and to the applied field (a higher field leads to an increased freezing temperature). Such a dependence is again absent from the magnetic behaviour of $(NH_3)K_3C_{60}$. Figure 6 presents an updated T_N versus volume per C_{60} molecule ($V \sim 1/W$) phase diagram of the ammoniated alkali fullerides to include the present results. The observed behaviour—namely, T_N first increases with interfullerene separation (increasing x), reaches a maximum and then decreases—is different from what is expected for a simple localized moment model (a continuous reduction of J and T_N as the interfullerene separation increases).

In order to understand the anomalous overall dependence of T_N on x, we recall an important structural difference between the members of the $(NH_3)K_{3-x}Rb_xC_{60}$ series. At room temperature, all these fullerides adopt an orthorhombic (space group *Fmmm*) structure. However, on cooling, they undergo a phase transition below $T_s \approx 150$ K, driven by the orientational ordering of both the alkali ion–ammonia pairs and the C_{60} units. The key observation is that the low-temperature orientationally ordered structures are not identical for all members of the series. For $0 \leqslant x \leqslant 2$, an orthorhombic (space group *Fddd*) superstructure is adopted with the K^+–NH_3 pairs ordering antiferroelectrically along the [110] direction, each chain rotated by 90° in consecutive planes along the *c*-axis (perpendicular ordering model) [15, 16]. On the other hand, for $2 < x \leqslant 3$, the orientational ordering motif is different—the $Rb(K)^+$–NH_3 pairs order antiferroelectrically along the [010] direction but chains are aligned parallel to each other in consecutive *ab* planes along the *c*-axis (parallel ordering model)—and the resulting superstructure has monoclinic (space group $C2/c$) symmetry [27, 28]. We propose that it is precisely this structural difference between $(NH_3)KRb_2C_{60}$ and $(NH_3)Rb_3C_{60}$ that is responsible for the anomalous suppression of T_N for the end members of the $(NH_3)K_{3-x}Rb_xC_{60}$ series despite the expansion in the interfullerene separation. Further evidence will have to await the detailed understanding at the microscopic level of the interfullerene exchange interactions in the two low-temperature superstructures.

Finally, it is of interest to compare the T_N values obtained for the $(NH_3)K_{3-x}Rb_xC_{60}$ systems with that of the recently synthesized methylaminated potassium fulleride, $(CH_3NH_2)K_3C_{60}$ [29]. For the latter compound, the volume per C_{60}^{3-} anion is comparable to

that in $(NH_3)KRb_2C_{60}$. Nevertheless, ZF μ^+SR and EPR data reveal that its T_N is reduced significantly to 11 K (open triangle in figure 6), consistent with much weaker interactions between the C_{60}^{3-} anions [30, 31]. Note that high-resolution x-ray diffraction data collected for $(CH_3NH_2)K_3C_{60}$ showed that its lattice expansion, compared to the pristine K_3C_{60} fulleride, is highly anisotropic (the C_{60}–C_{60} long/short contact exceeds sufficiently those obtained for the $(NH_3)K_{3-x}Rb_xC_{60}$ analogues), accompanied also by the introduction of C_{60}–H–C interactions [29]. These structural characteristics and the possibly different orientational ground state of the fullerene molecules (different exchange interactions) could explain the strong T_N reduction in the methylaminated potassium fulleride as compared to the ammoniated alkali fullerides investigated here.

4. Conclusions

In conclusion, μ^+SR spectroscopy on the $(NH_3)K_{3-x}Rb_xC_{60}$ ($0 \leqslant x \leqslant 3$) fullerides confirms that the AF state is their common low-temperature electronic ground state, characterized by local fields of quasi-static nature with large spatial inhomogeneities. A large fraction of paramagnetic domains survives well into the AF state. The cooling protocol of the larger ammoniated alkali fullerides plays an important role in the appearance of coherent ordering of the magnetic moments, presumably due to the enhanced orientational disorder of the C_{60}^{3-} ions at rapid cooling rates and the consequent suppression of the intermolecular exchange interactions. The Néel temperatures in the series of ammoniated alkali fullerides increase monotonically with x (lattice expansion) on going from $x = 0$ to 2 and then decrease in the most expanded $(NH_3)Rb_3C_{60}$ member. The origin of the observed anomalous T_N versus x dependence should be related to the differing low-temperature orientational ordering structural motifs across the series.

Acknowledgments

This work has been supported by EPSRC (KP/MJR) and by a Marie Curie European reintegration grant under contract number MERG-CT-2004-513606 (JA). The authors thank the Paul Scherrer Institute for provision of muon beamtime and A Amato for help with the experiments.

References

[1] Tanigaki K, Ebbesen T W, Saito S, Mizuki J, Tsai J S, Kubo Y and Kuroshima S 1991 *Nature* **352** 222
[2] Palstra T T M, Zhou O, Iwasa Y, Sulewski P E, Fleming R M and Zegarski B R 1995 *Solid State Commun.* **93** 327
[3] Gunnarsson O 2004 *Alkali-Doped Fullerides* (Singapore: World Scientific)
[4] Margadonna S and Prassides K 2002 *J. Solid State Chem.* **168** 639
[5] Durand P, Darling G R, Dubitsky Y, Zaopo A and Rosseinsky M J 2003 *Nat. Mater.* **2** 605
[6] Iwasa Y and Takenobu T 2003 *J. Phys.: Condens. Matter* **15** R495
[7] Koch E, Gunnarson O and Martin R M 1999 *Phys. Rev. Lett.* **83** 620
[8] Rosseinsky M J, Murphy D W, Fleming R M and Zhou O 1993 *Nature* **364** 425
[9] Iwasa Y, Shimoda H, Palstra T T M, Maniwa Y, Zhou O and Mitani T 1996 *Phys. Rev.* B **53** 8836
[10] Allen K M, Heyes S J and Rosseinsky M J 1996 *J. Mater. Chem.* **6** 1445
[11] Simon F, Janossy A, Muranyi F, Feher T, Shimoda H, Iwasa Y and Forro L 2000 *Phys. Rev.* B **61** 3826
[12] Kitano H, Matsuo R, Miwa K, Maeda A, Takenobu T, Iwasa Y and Mitani T 2002 *Phys. Rev. Lett.* **88** 096401
[13] Tou H, Maniwa Y, Iwasa Y, Shimoda H and Mitani T 2000 *Phys. Rev.* B **62** 775
[14] Prassides K, Margadonna S, Arcon D, Lappas A, Shimoda H and Iwasa Y 1999 *J. Am. Chem. Soc.* **121** 11227

[15] Ishii K, Watanuki T, Fujiwara A, Suematsu H, Iwasa Y, Shimoda H, Mitani T, Nakao H, Fujii Y, Murakami Y and Kawada H 1999 *Phys. Rev.* B **59** 3596
[16] Margadonna S, Prassides K, Shimoda H, Takenobu T and Iwasa Y 2001 *Phys. Rev.* B **64** 132414
[17] Takenobu T, Muro T, Iwasa Y and Mitani T 2000 *Phys. Rev. Lett.* **85** 381
[18] Moriya T and Hasegawa H 1980 *J. Phys. Soc. Japan* **48** 1490
[19] Schenck A 1993 *Frontiers in Solid State Sciences: Magnetism* vol 2, ed L C Cupta and M S Murani (Singapore: World Scientific)
[20] Lappas A, Prassides K, Vavekis K, Arcon D, Blinc R, Cevc P, Amato A, Feyerherm R, Gygax F N and Schenck A 1995 *Science* **267** 1799
[21] Kubo R and Toyabe T 1967 *Magnetic Resonance and Relaxation* ed R Blinc (Amsterdam: North-Holland) pp 810–23
[22] Hayano R S, Uemura Y J, Imazato J, Nishida N, Yamazaki T and Kubo R 1979 *Phys. Rev.* B **20** 850
[23] Schenck A and Gygax F N 1995 *Handbook of Magnetic Materials* vol 9, ed K H J Buskhow (Amsterdam: Elsevier)
[24] Prassides K, Tanigaki K and Iwasa Y 1997 *Physica* C **282** 307
[25] Collins M F 1989 *Magnetic Critical Scattering* (Oxford: Oxford University Press)
[26] de Jongh L J and Miedema A R 1974 *Adv. Phys.* **23** 1
[27] Margadonna S, Iwasa Y, Takenobu T and Prassides K 2004 *Struct. Bonding* **109** 127
[28] Margadonna S 2002 *New Diamond Front. Carbon Technol.* **12** 287
[29] Ganin A Y, Takabayashi Y, Bridges C A, Khimyak Y Z, Margadonna S, Prassides K and Rosseinsky M J 2006 *J. Am. Chem. Soc.* **128** 14784
[30] Takabayashi Y, Ganin A Y, Rosseinsky M J and Prassides K 2007 *Chem. Commun.* 870
[31] Ganin A Y, Takabayashi Y, Pregelj M, Zorko A, Arcon A, Rosseinsky M J and Prassides K 2007 *Chem. Mater.* **19** 3177